Available online at www.sciencedirect.com
ScienceDirect
Journal of the European Ceramic Society 30 (2010) 2707–2713
www.elsevier.com/locate/jeurceramsoc

Technical note

High-temperature hot corrosion behavior of gadolinium zirconate by vanadium pentoxide and sodium sulfate in air

Zhan-Guo Liu, Jia-Hu Ouyang *, Yu Zhou, Sa Li

Institute for Advanced Ceramics, Department of Materials Science, Harbin Institute of Technology, No. 92, West Da-Zhi Street, Harbin 150001, China

Received 5 November 2009; received in revised form 23 April 2010; accepted 4 May 2010

Abstract

Gadolinium zirconate ($Gd_2Zr_2O_7$) prepared by solid state reaction exhibited a defect fluorite-type structure. Reactions between $Gd_2Zr_2O_7$ ceramic and vanadium pentoxide (V_2O_5), sodium sulfate (Na_2SO_4), and $V_2O_5 + Na_2SO_4$ mixture were investigated from 700 to 1000 °C in air using an X-ray diffractometer (XRD), scanning electron microscopy (SEM) and energy-dispersive X-ray spectroscopy (EDS). V_2O_5 reacts with $Gd_2Zr_2O_7$ to form gadolinium vanadate ($GdVO_4$) and monoclinic zirconia (*m*-ZrO_2) at 900 and 1000 °C in air. However, no chemical reaction product between Na_2SO_4 and $Gd_2Zr_2O_7$ is found at 900 and 1000 °C in air. V_2O_5 reacts with equal molar Na_2SO_4 to form sodium vanadate ($NaVO_3$) at 610 °C. In the temperature range of 700–1000 °C, $Na_2SO_4 + V_2O_5$ mixture reacts with $Gd_2Zr_2O_7$ in air to form the final reaction products of $GdVO_4$ and *m*-ZrO_2.

Keywords: $Gd_2Zr_2O_7$; Hot corrosion; V_2O_5; Na_2SO_4

1. Introduction

Thermal barrier coatings (TBCs) are extensively used to insulate metallic components against hot gas stream, and have become a critical technology for improving performance of gas-turbine engines.[1–3] TBCs systems typically consist of a metallic oxidation protection layer and a thermally insulative ceramic topcoat. The state of the art topcoat material is 6–8 wt.% yttria-stabilized zirconia (YSZ), which is generally produced by plasma spraying (PS) or electron beam physical vapor deposition (EB-PVD).[4] However, YSZ is limited to applications below 1200 °C.[5] Above 1200 °C, the *t*′-phase zirconia transforms into cubic and tetragonal phases. During cooling the tetragonal phase will further transform into the monoclinic phase, which is accompanied with a volume change of 3–5% and a severe damage of TBCs.[4–7]

In recent years, there is an increasing demand for developing new design strategies or new materials for TBCs in order to address the challenges of more demanding operating environments. Among high-melting ceramic materials, rare-earth zirconates with the general formula $Ln_2Zr_2O_7$ (Ln = lanthanide) have been shown to posses some very important properties for TBCs application. The thermal conductivities of rare-earth zirconates varied from 1.1 to 2.0 $W\,m^{-1}\,K^{-1}$ in the temperature range of room temperature to 1400 °C.[8–12] In addition, the phase transition temperatures of rare-earth zirconates are clearly higher than the *t*-*m* phase transformation temperature of YSZ, such as 2300 °C for $Nd_2Zr_2O_7$, 2000 °C for $Sm_2Zr_2O_7$, and 1530 °C for $Gd_2Zr_2O_7$, respectively.[13] $Gd_2Zr_2O_7$-based zirconates are a class of potential candidate materials for high-temperature TBCs applications (temperature above 1150 °C) instead of currently used YSZ TBCs, where both hot corrosion and oxidation reaction are a great concern.[10] When TBCs are operated with low-quality fuels containing appreciable levels of vanadium, sodium, sulfur, etc, the hot corrosion of ceramic topcoat becomes significant at elevated temperatures.[14] Mohan et al. tested the degradation of YSZ coatings by molten Na_2SO_4 at a temperature range from 900 to 1200 °C.[15] Chen et al. found that the penetration of molten V_2O_5 into YSZ coatings were quite deleterious to ceramic topcoat and lead to the formation of $LaVO_4$ and m-ZrO_2 from 800 to 1200 °C.[16,17] In our previous work, V_2O_5 reacted with $Gd_2Zr_2O_7$ at 700–850 °C.[18] Molten V_2O_5 reacted

* Corresponding author at: Harbin Institute of Technology, Dept. Materials Science, PO Box 433, 92 Westdazhi Street, Nangang Dist., Harbin, Heilongjiang 150001, China. Tel.: +86 451 86414291; fax: +86 451 86414291.
E-mail address: ouyangjh@hit.edu.cn (J.-H. Ouyang).

0955-2219/$ – see front matter © 2010 Elsevier Ltd. All rights reserved.
doi:10.1016/j.jeurceramsoc.2010.05.002

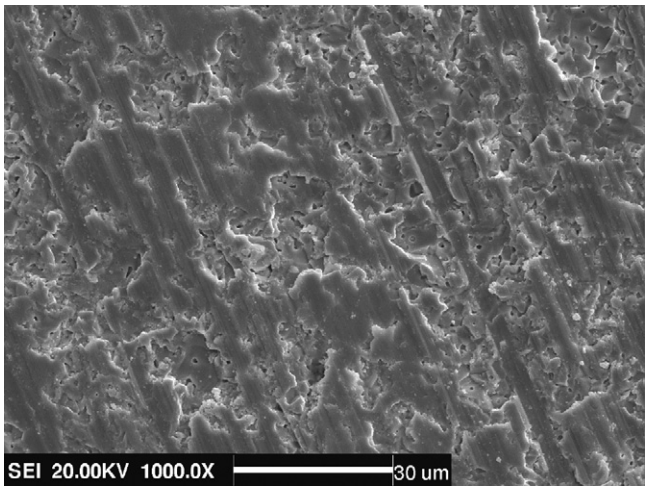

Fig. 1. Surface morphology of unpolished $Gd_2Zr_2O_7$ ceramic sintered at 1650 °C for 10 h in air.

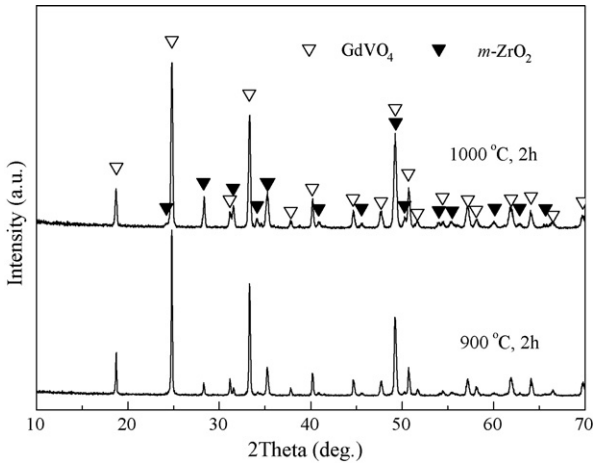

Fig. 2. X-ray diffraction patterns of V_2O_5-coated $Gd_2Zr_2O_7$ specimen heat-treated at 900 °C and 1000 °C for 2 h in air.

with $Gd_2Zr_2O_7$ to form ZrV_2O_7 and $GdVO_4$ at 700 °C; however, in a temperature range of 750–850 °C, molten V_2O_5 reacted with $Gd_2Zr_2O_7$ to form $GdVO_4$ and *m*-ZrO_2. For a comparative study, Marple et al. investigated the hot corrosion behavior of $La_2Zr_2O_7$ and YSZ coatings to vanadium- and sulfur-containing compounds at 900 and 1000 °C, respectively.[19] $La_2Zr_2O_7$ coatings had a relatively high corrosion resistance to the attack by molten V_2O_5. $La_2Zr_2O_7$ coatings remained well bonded to the substrate after exposure to V_2O_5, and formed only minor amounts of $LaVO_4$. However, $La_2Zr_2O_7$ coatings in contact with sulfate salts ($3Na_2SO_4$:$2MgSO_4$) at 900 °C exhibited a very rapid disintegration of coatings to form $La_2O_2SO_4$, MgO and *m*-ZrO_2 under a gas flow consisting of 2000 mL/min of dried air and 5 mL/min of SO_2.[19] The YSZ coatings after thermal exposure to vanadia formed a mixture of YVO_4 and monoclinic ZrO_2, which resulted in increased microcracking and spallation of ceramic topcoat. However, YSZ coatings exhibited an excellent resistance to the attack by sulfate salts. When $La_2Zr_2O_7$ and YSZ coatings were exposed to a mixture of vanadia and sulfate salts, both coatings were degraded, the YSZ by vanadia and the $La_2Zr_2O_7$ by the sulfate.[19] In the present study, in order to investigate the hot corrosion behavior of $Gd_2Zr_2O_7$ ceramic by V_2O_5 at elevated temperatures, Na_2SO_4 and $V_2O_5 + Na_2SO_4$ mixture, hot corrosion experiments were performed at different temperature up to 1000 °C for 2 h in air.

2. Experimental procedure

In the present study, $Gd_2Zr_2O_7$ was prepared by a solid state reaction process. Details of the sample preparation can be found in our previous work.[18] XRD measurement shows that $Gd_2Zr_2O_7$ has a single phase of defect fluorite-type structure. The specimens with dimensions of 10 mm × 10 mm × 2 mm were ultrasonically degreased in acetone, and dried at 100 °C in oven. These specimens, in contact with three kinds of different salts, namely V_2O_5, Na_2SO_4, and $Na_2SO_4 + V_2O_5$ mixture (50–50 mol.%), were isothermally heat-treated at different temperatures ranging from 700 to 1000 °C for 2 h in air. During hot corrosion test, the salts were spread uniformly over the surface of $Gd_2Zr_2O_7$ specimen at a concentration of 15 mg/cm^2 by using a very fine glass rod cleaned and dried ultrasonically.

Crystal structures of hot corrosion specimens were identified by an X-ray diffractometer (XRD, D/Max-2200VPC, Rigaku Co. Ltd., Japan) with Cu *K*α radiation at a scan rate of 3°/min. The microstructural analysis of hot corrosion specimens was carried out with a scanning electron microscope (SEM, Cam-Scan MX 2600FE, UK) equipped with energy-dispersive X-ray

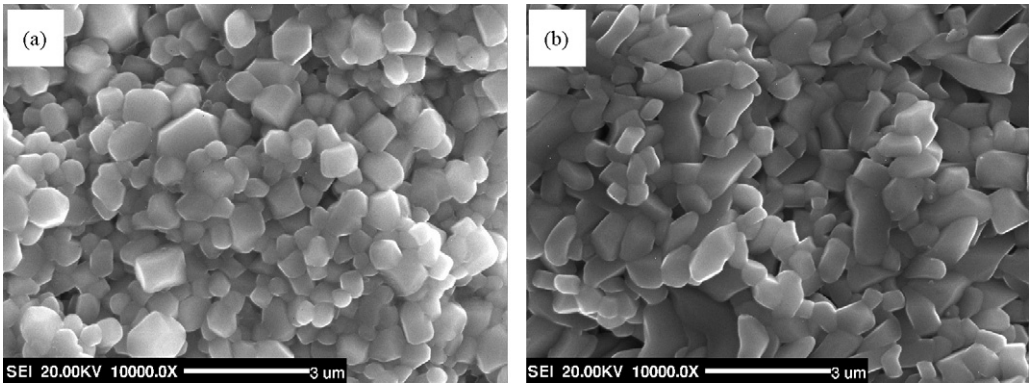

Fig. 3. Microstructure of V_2O_5-coated $Gd_2Zr_2O_7$ specimens heat-treated at different temperatures for 2 h in air: (a) 900 °C; (b) 1000 °C.

spectroscopy (EDS, Oxford Instruments INCA X-sight system, 7537, UK) operating at 20 kV. A thin carbon coating was evaporated onto the surface of the specimens for electrical conductivity.

3. Results and discussion

Fig. 1 shows the surface morphology of unpolished $Gd_2Zr_2O_7$ ceramic sintered at 1650 °C for 10 h in air. There are some small pores in the specimen. Fig. 2 shows XRD patterns obtained from the V_2O_5-coated $Gd_2Zr_2O_7$ specimen heat-treated at 900 and 1000 °C for 2 h in air. The newly evolved peaks are due to two different reaction products, *m*-ZrO_2 (JCPDS no. 37–1484) and $GdVO_4$ (JCPDS no. 17–0260). The phase constituents of the V_2O_5-coated $Gd_2Zr_2O_7$ specimens heat-treated at 900 and 1000 °C for 2 h are consistent with the results obtained at 750–850 °C for 2 h, which was reported in our previous work.[18] Typical surface morphology of the V_2O_5-coated $Gd_2Zr_2O_7$ specimen heat-treated at 900 and 1000 °C for 2 h is shown in Fig. 3. From Fig. 3, the microstructure after heat-treatments at 900 and 1000 °C for 2 h is very similar to those obtained at 750–850 °C for 2 h.[18]

The melting point of Na_2SO_4 is 884 °C. In this study, hot corrosion tests of $Gd_2Zr_2O_7$ specimens with Na_2SO_4 were performed at 900 and 1000 °C for 2 h, respectively. XRD patterns obtained from the Na_2SO_4-coated $Gd_2Zr_2O_7$ specimens heat-treated at 900 and 1000 °C for 2 h in air are shown in Fig. 4. There are only original Na_2SO_4 and $Gd_2Zr_2O_7$ phases, and no new reaction product was found from these XRD spectra. It indicates that no chemical reaction takes place between Na_2SO_4 and $Gd_2Zr_2O_7$ at 900 and 1000 °C for 2 h in air. Fig. 5 shows the microstructure of the Na_2SO_4-coated $Gd_2Zr_2O_7$ specimen heat-treated at 900 °C for 2 h in air. The EDS spectra obtained at different regions of A and B in Fig. 5(b) confirm the presence of elements consistent with $Gd_2Zr_2O_7$ (region A) and Na_2SO_4 (region B) as shown in Fig. 5(c) and (d). Microstructure of Na_2SO_4-coated $Gd_2Zr_2O_7$ specimen heat-treated at 1000 °C for 2 h in air is shown in Fig. 6. From Fig. 6(b), it is clearly seen that

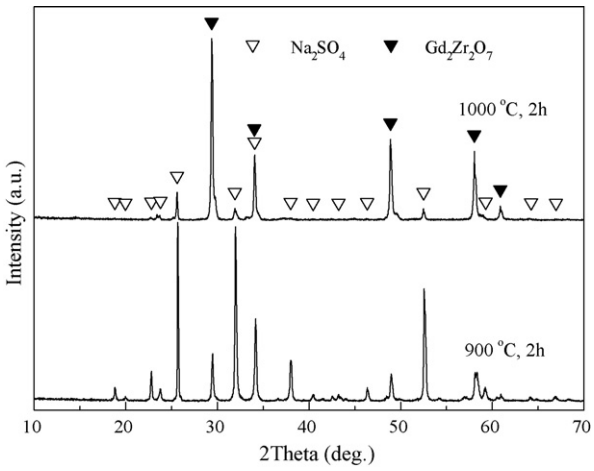

Fig. 4. X-ray diffraction patterns of Na_2SO_4-coated $Gd_2Zr_2O_7$ specimen heat-treated at 900 °C and 1000 °C for 2 h in air.

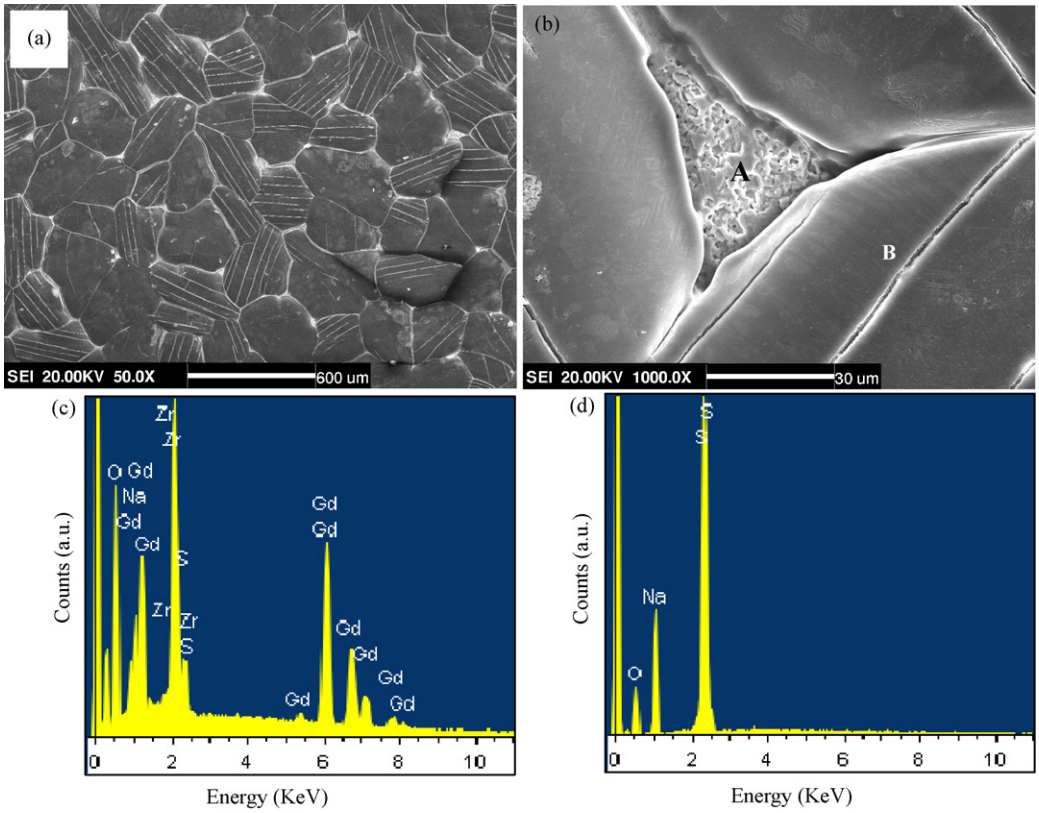

Fig. 5. Microstructure of Na_2SO_4-coated $Gd_2Zr_2O_7$ specimens heat-treated at 900 °C for 2 h in air: (a) low-magnification micrograph; (b) high-magnification micrograph; (c and d) EDS spectra at the locations of A and B in (b), respectively.

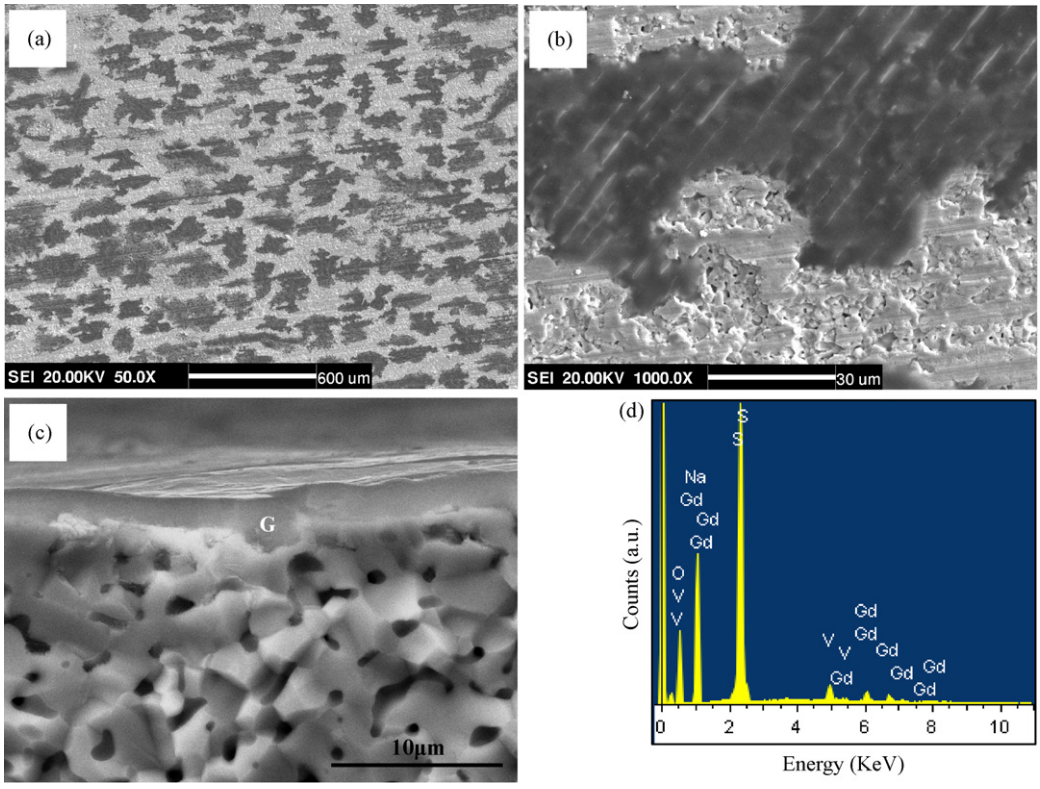

Fig. 6. Microstructure of Na_2SO_4-coated $Gd_2Zr_2O_7$ specimen heat-treated at 1000 °C for 2 h in air: (a) low-magnification image; (b) high-magnification image; (c) fractured cross-section; (d) EDS spectra at the locations of G in (c).

the morphologies of $Gd_2Zr_2O_7$ and Na_2SO_4 are similar to those in Fig. 1 and Fig. 5(a), respectively. As the melting point and boiling point of Na_2SO_4 is 884 °C and 1404 °C, respectively, some of molten Na_2SO_4 may evaporate after thermal exposure to higher temperatures of 900 and 1000 °C. From Figs. 5 and 6, molten Na_2SO_4 still remains on the corroded surface after thermal exposure to 900 and 1000 °C. Fig. 6(c) is the cross-section micrograph of the fractured surface after thermal exposure to 1000 °C, which further proves the presence of Na_2SO_4 by EDS analysis (Fig. 6(d)) of the location G at the top surface layer. However, from Fig. 4, the evaporation of Na_2SO_4 occurs more at 1000 °C clearly, which is coincident with the peak intensity of sulfate phase in the XRD pattern, although some of them also penetrate into the ceramic substrate.

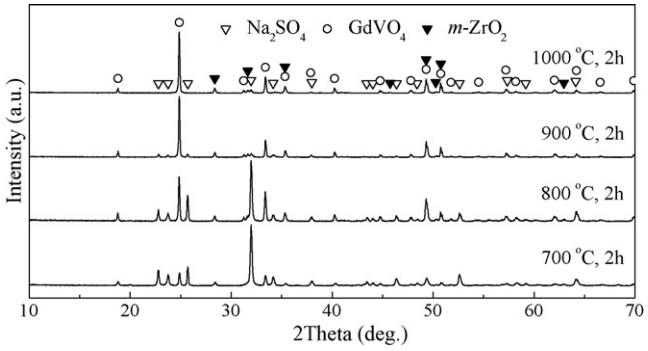

Fig. 7. X-ray diffraction patterns of $Na_2SO_4 + V_2O_5$-coated $Gd_2Zr_2O_7$ specimens heat-treated at 700–1000 °C for 2 h in air.

Fig. 7 shows XRD patterns obtained from the $Gd_2Zr_2O_7$ specimens coated with a $Na_2SO_4 + V_2O_5$ mixture heat-treated at 700–1000 °C for 2 h in air. No V_2O_5 phase is found from the XRD analysis. Besides unreacted Na_2SO_4, *m*-ZrO_2 and $GdVO_4$ are found to exist after chemical reaction at 700–1000 °C for 2 h in air. Fig. 8 shows the microstructure of the $Gd_2Zr_2O_7$ specimens coated with $Na_2SO_4 + V_2O_5$ mixture heat-treated at 700 °C for 2 h in air. From the EDS results in Fig. 8(c) and (d) obtained at different regions in Fig. 8(b), the region C contains reaction products of both $GdVO_4$ and a very small quantity of *m*-ZrO_2, while the region D is composed of the original Na_2SO_4. Typical microstructure of the $Gd_2Zr_2O_7$ specimens coated with $Na_2SO_4 + V_2O_5$ mixture heat-treated at 800 and 900 °C for 2 h in air is shown in Fig. 9. Clearly, there are lots of Na_2SO_4 on the specimen surface. The surface morphology of $Gd_2Zr_2O_7$ specimen coated with $Na_2SO_4 + V_2O_5$ mixture heat-treated at 1000 °C for 2 h in air is presented in Fig. 10. The EDS spectra obtained at different regions of E and F in Fig. 10 (b) confirm the presence of elements consistent with *m*-ZrO_2 (region E) and $GdVO_4$ (region F) as shown in Fig. 10(c) and (d).

Na_2SO_4 itself does not react with $Gd_2Zr_2O_7$ at 900 and 1000 °C for 2 h in air. However, $Na_2SO_4 + V_2O_5$ mixture reacts with $Gd_2Zr_2O_7$ to form *m*-ZrO_2 and $GdVO_4$ at 700–1000 °C for 2 h in air. According to the phase diagram in the Na_2SO_4–V_2O_5 binary system, the equal molar of Na_2SO_4 and V_2O_5 has a chemical reaction to form sodium vanadate ($NaVO_3$) at 610 °C.[20] The reaction mechanism is given by the following chemical equation:

$$Na_2SO_4(l) + V_2O_5(l) \rightarrow NaVO_3(l) + SO_3(g) \quad (1)$$

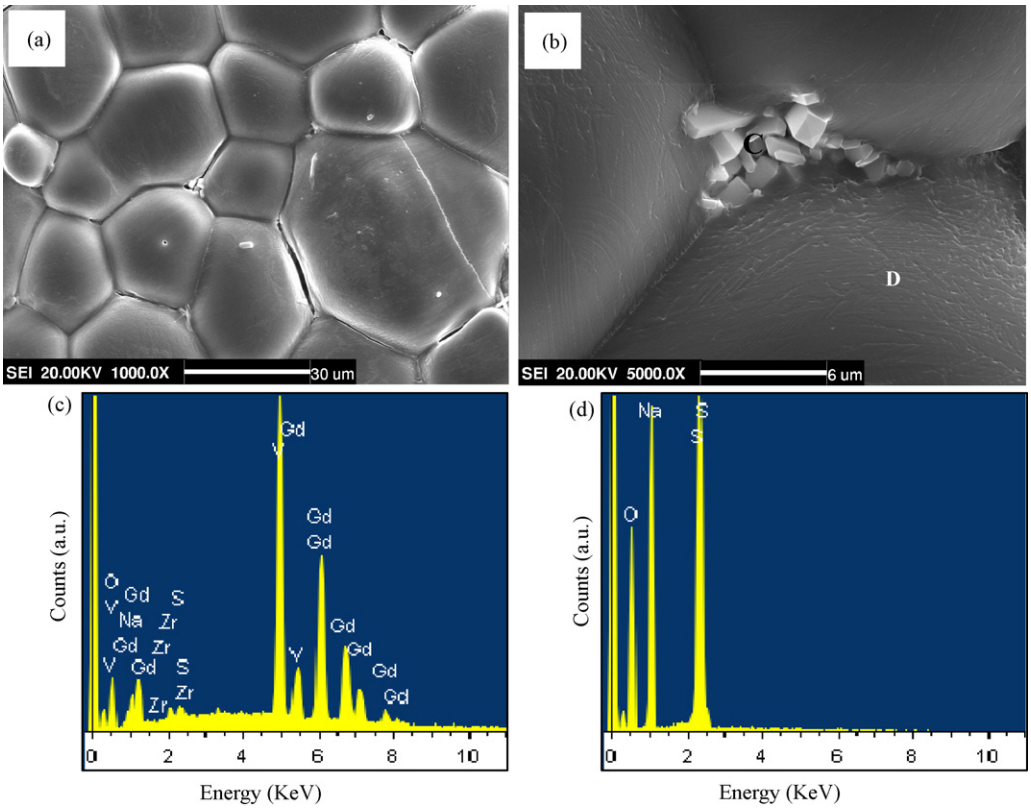

Fig. 8. Microstructure of the $Gd_2Zr_2O_7$ specimens coated with $Na_2SO_4 + V_2O_5$ mixture heat-treated at 700 °C for 2 h in air: (a) low-magnification micrograph; (b) high-magnification micrograph; (c and d) EDS spectra at the locations of C and D in (b), respectively.

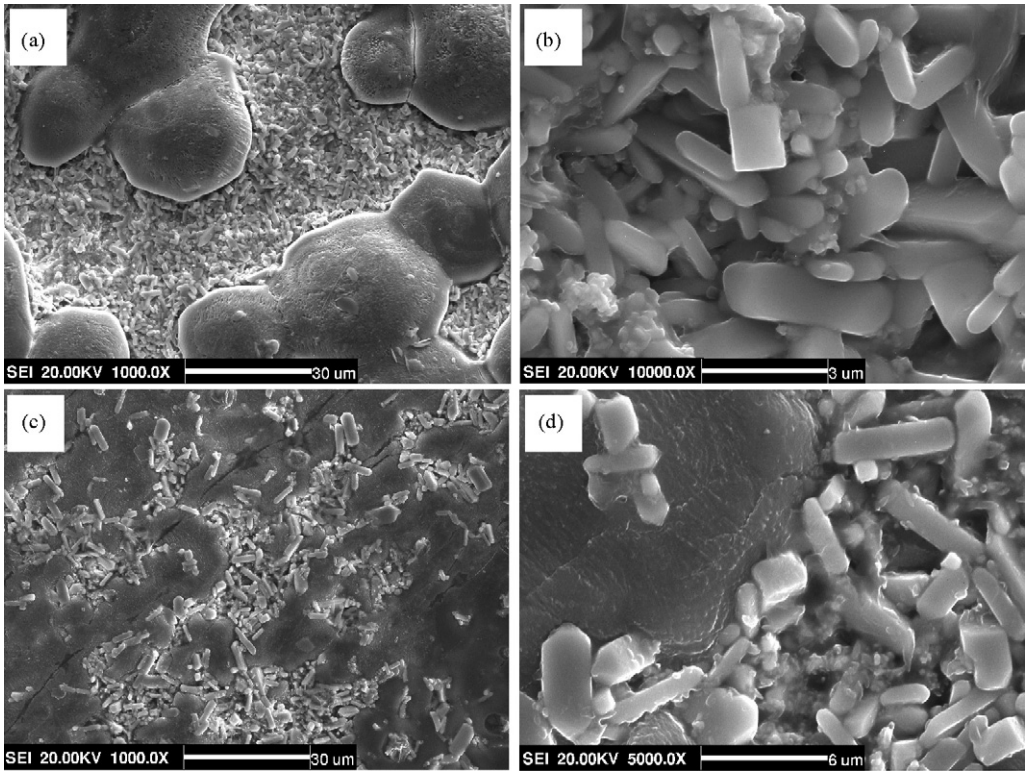

Fig. 9. Microstructure of the $Gd_2Zr_2O_7$ specimens coated with $Na_2SO_4 + V_2O_5$ mixture heat-treated at 800 and 900 °C for 2 h in air: (a and c) low-magnification micrograph after heat treatment at 800 °C and 900 °C for 2 h, respectively; (b and d) corresponding high-magnification micrograph of (a) and (c), respectively.

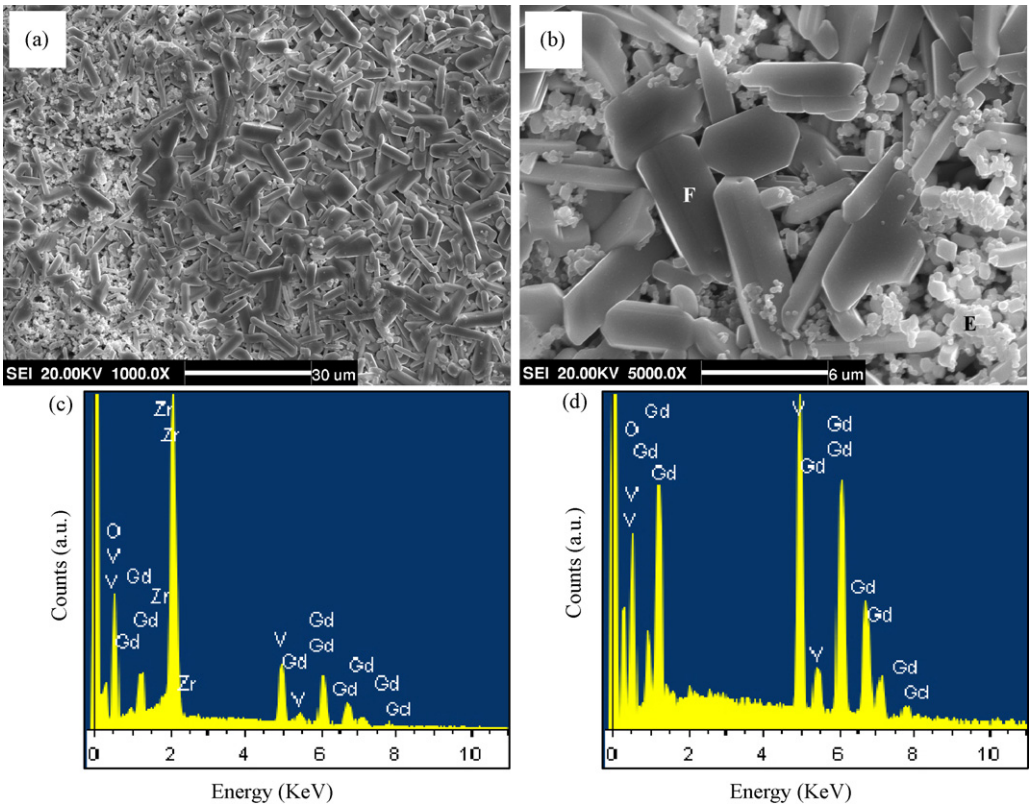

Fig. 10. Microstructure of the $Gd_2Zr_2O_7$ specimens coated with $Na_2SO_4 + V_2O_5$ mixture heat-treated at 1000 °C for 2 h in air: (a) low-magnification micrograph; (b) high-magnification micrograph; (c and d) EDS spectra at the locations of E and F in (b), respectively.

At the same time, $NaVO_3$ continues to react with $Gd_2Zr_2O_7$ ceramic to form the final reaction products of $GdVO_4$ and *m*-ZrO_2. The reaction mechanism is given by the following chemical equation:

$$NaVO_3(l) + Gd_2Zr_2O_7(s) \rightarrow 2GdVO_4(s) + 2m\text{-}ZrO_2(s) + Na_2O(l) \quad (2)$$

4. Summary

$Gd_2Zr_2O_7$ ceramic prepared by pressureless-sintering process has been subjected to isothermal air furnace testing in the presence of V_2O_5, Na_2SO_4, and $V_2O_5 + Na_2SO_4$ mixture (50–50 mol.%). V_2O_5 reacts with $Gd_2Zr_2O_7$ ceramic to form $GdVO_4$ and *m*-ZrO_2 at 900 and 1000 °C in air. No chemical reaction between Na_2SO_4 and $Gd_2Zr_2O_7$ is found at 900 and 1000 °C in air. However, V_2O_5 reacts with equal molar Na_2SO_4 to form $NaVO_3$ at 610 °C. In the temperature range of 700–1000 °C, $Na_2SO_4 + V_2O_5$ mixture reacts with $Gd_2Zr_2O_7$ ceramic to form the final reaction products of $GdVO_4$ and *m*-ZrO_2.

Acknowledgements

The authors would like to thank the financial support from the National Natural Science Foundation of China (NSFC-no. 50972030).

References

[1]. Padture NP, Gell M, Jordan EH. Thermal barrier coatings for gas-turbine engine applications. *Science* 2002;**296**:280–4.
[2]. Cao XQ, Vassen R, Stőver D. Ceramic materials for thermal barrier coatings. *J Eur Ceram Soc* 2004;**24**:1–10.
[3]. Vaßen R, Cernuschi F, Rizzi G, Scrivani A, Markocsan N, Östergren L, et al. Recent activities in the field of thermal barrier coatings including burner rig testing in the European union. *Adv Eng Mater* 2008;**10**:907–21.
[4]. Cao XQ. Application of rare earths in thermal barrier coating materials. *J Mater Sci Technol* 2007;**23**:15–35.
[5]. Vassen R, Stuke A, Stöver D. Recent developments in the field of thermal barrier coatings. *J Therm Spray Technol* 2009;**18**:181–6.
[6]. Evans AG, Clarke DR, Levi CG. The influence of oxides on the performance of advanced gas turbines. *J Eur Ceram Soc* 2008;**28**:1405–19.
[7]. Andrievskaya ER. Phase equilibria in the refractory oxide systems of zirconia, hafnia and yttria with rare-earth oxides. *J Eur Ceram Soc* 2008;**28**:2363–88.
[8]. Vassen R, Cao X, Tietz F, Basu D, Stőver D. Zirconates as new materials for thermal barrier coatings. *J Am Ceram Soc* 2000;**83**:2023–8.
[9]. Wu J, Wei XZ, Padture NP, Klemens PG, Gell M, Garcia E, et al. Low-thermal-conductivity rare-earth zirconates for potential thermal-barrier-coating applications. *J Am Ceram Soc* 2002;**85**:3031–5.
[10]. Lehmann H, Pitzer D, Pracht G, Vassen R, Stőver D. Thermal conductivity and thermal expansion coefficients of the lanthanum rare-earth-element zirconate system. *J Am Ceram Soc* 2003;**86**:1338–44.
[11]. Liu Z-G, Ouyang J-H, Zhou Y, Meng QC, Xia X-L. Order–disorder transition and thermal conductivity of $(Yb_xNd_{1-x})_2Zr_2O_7$ solid solutions. *Phil Mag* 2009;**89**:553–64.
[12]. Liu Z-G, Ouyang J-H, Zhou Y, Li J, Xia X-L. Influence of ytterbium- and samarium-oxides codoping on structure and thermal conductivity of zirconate ceramics. *J Eur Ceram Soc* 2009;**29**:647–52.

[13]. Michel D, Perez-y-Jorba M, Collongues R. Etude de la transformation ordre–desordre de la structure fluorite a la structure pyrochlore pour des phases $(1-x)ZrO_2$–xLn_2O_3. *Mater Res Bull* 1974;**9**:1457–68.

[14]. Bose S. *High temperature coatings*. Burlington: Elsevier Inc.; 2007. p. 55–70.

[15]. Mohan P, Yuan B, Patterson T, Desai VH, Sohnw YH. Degradation of yttria-stabilized zirconia thermal barrier coatings by vanadium pentoxide, phosphorous pentoxide, and sodium sulfate. *J Am Ceram Soc* 2007;**90**:3601–7.

[16]. Chen Z, Speakman S, Howe J, Wang H, Porter W, Trice R. Investigation of reactions between vanadium oxide and plasma-sprayed yttria-stabilized zirconia coatings. *J Eur Ceram Soc* 2009;**29**:1403–11.

[17]. Chen Z, Mabon J, Wen J-G, Trice R. Degradation of plasma-sprayed yttria-stabilized zirconia coatings via ingress of vanadium oxide. *J Eur Ceram Soc* 2009;**29**:1647–56.

[18]. Liu Z-G, Ouyang J-H, Zhou Y, Xia X-L. Hot corrosion behavior of V_2O_5-coated $Gd_2Zr_2O_7$ ceramic in air at 700–850 °C. *J Eur Ceram Soc* 2009;**29**:2423–7.

[19]. Marple BR, Voyer J, Thibodeau M, Nagy DR, Vassen R. Hot corrosion of lanthanum zirconate and partially stabilized zirconia thermal barrier coatings. *J Eng Gas Turb Power* 2006;**128**:144–52.

[20]. In: Smith G, editor. *Phase diagrams for ceramists*, vol. IV. Columbus, OH: American Ceramic Society; 1981 [Fig. 5127].